Tetrahedron 71 (2015) 6409–6413

Contents lists available at ScienceDirect

Tetrahedron

journal homepage: www.elsevier.com/locate/tet

Branched/linear selectivity in palladium-catalyzed allyl-allyl cross-couplings: the role of ligands☆

Michael J. Ardolino, James P. Morken *

Department of Chemistry, Boston College, Chestnut Hill, MA 02467, USA

ARTICLE INFO

Article history:
Received 12 March 2015
Received in revised form 1 May 2015
Accepted 5 May 2015
Available online 15 May 2015

Keywords:
Bite angle
Cross-coupling
Allylation
Pd catalysis

ABSTRACT

While Pd-catalyzed allyl-allyl cross-couplings in the presence of small-bite-angle bidentate ligands reliably furnish the branched regioisomer with high levels of selectivity, cross-couplings in the presence of large-bite-angle bidentate ligands give varying, often unpredictable, levels of selectivity. In a combined computational and experimental study, we probe the underlying features that govern the regioselectivity in these metal-catalyzed cross-couplings.

1. Introduction

The transition metal-catalyzed coupling of two allylic fragments has the power to generate synthetically useful 1,5-dienes from an allylic electrophile and allylic nucleophile (Scheme 1).[1] Under palladium catalysis, the allyl-allyl coupling reaction has been known for some time and typically yields linear, achiral dienes of type **A** with monodentate phosphine ligands (Eq 1).[2] Recently, our group has disclosed a number of methods that employ chiral, small-bite-angle bidentate phosphine ligands to reverse the regioselectivity of these couplings to give branched 1,5-dienes of type **C** with excellent regio- and enantioselectivity (Eq 2).[3] Recent mechanistic and computational studies[4] have supported previous proposals[3] that the reaction is operative through an inner-sphere 3,3′-reductive elimination,[5] in which coupling at carbons 3 and 3′ through the conformation as shown in **B** leads to the branched isomer. These studies are in line with computational studies on the preferred reductive elimination pathways for unsubstituted allylic systems by Eschavarren[5a] and Espinet,[5c] which also found the 3,3′-reductive elimination to be preferred over direct coupling at the 1 and 1′ carbons.

Although our previous study provided a deeper understanding of the origins of branched regioselectivity for small-bite-angle bidentate phosphine ligands, it did not explain trends in regioselectivity that we have observed with other ligands.[3a] As seen in

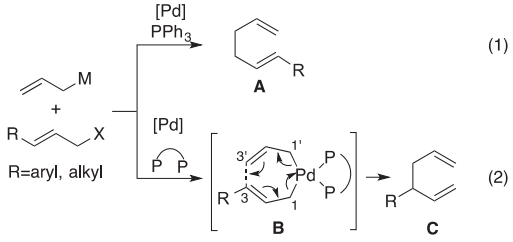

Scheme 1. Linear/branched selectivity in allyl-allyl coupling.

Table 1 and in line with previous studies, use of PPh_3 as the ligand in the Pd-catalyzed coupling of cinnamyl *t*-butyl carbonate **1** and allyl B(pin) **2** (entry 1) gives high selectivity for the linear 1,5-diene **4**. Ligands with smaller bite-angles (entries 2–4) gave high branched selectivity, however, selectivity became unpredictable as the bite-angle increased (entries 6–8).[6] Unable to explain the source of such disparate regioselectivity in systems containing either monodentate or wide-bite-angle bidentate ligands, we undertook additional mechanistic and computational studies to probe the origins of linear selectivity.[7]

2. Results and discussion

2.1. Monodentate ligands

To explore the source of high linear regioselectivity in Pd-catalyzed allyl-allyl couplings with monodentate ligands,

☆ This article is submitted with a hearty congratulations to Professor Tsuji on receipt of the 2014 Tetrahedron Prize for Creativity in Organic Chemistry!

* Corresponding author. Tel.: +1 627 552 6290; e-mail address: morken@bc.edu (J.P. Morken).

http://dx.doi.org/10.1016/j.tet.2015.05.015
0040-4020/

Table 1
Impact of ligand structure on cross coupling selectivity[a]

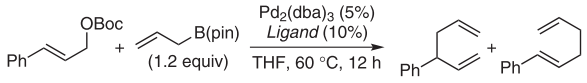

Entry	Ligand	B_n(°)	Yield (%)	b:l (**3**:**4**)
1	PPh_3	—	96	1:>20
2	dppbenzene	83	70	97:3
3	dppe	85	77	98:2
4	dppp	91	80	97:3
5	dppf	96	43	94:6
6	dppb	98	77	38:62
7	DPEphos	102	58	72:28
8	Xantphos	109	>95% conv.	53:47

[a] Data in entries 1–7 from ref. 3a.

computational studies utilizing density functional theory (DFT) were carried out.[8] These studies considered possible pathways leading to linear and branched isomers of phenyl-substituted 1,5-diene products of type **3** and **4** (Table 1), and began from the bis-ligated, bis(η^1-allyl) complex $\mathbf{GS_A}$ (Fig. 1). Based on previous studies,[5a,c] the two lowest energy routes for bond formation from $\mathbf{GS_A}$ should be through coupling at the either 3 and 3′ ($\mathbf{TS_A}$) or 1 and 1′ carbons ($\mathbf{TS_B}$). The 3,3′-pathway to give the branched isomer **3** ($\mathbf{TS_A}$) was calculated to have an activation free energy barrier of 14.6 kcal/mol. The alternate 1,1′-coupling to give linear product ($\mathbf{TS_B}$), lies 5.5 kcal/mol higher in energy, making it an unlikely source of **4**. An alternate route to this linear product could be 3,3′ reductive elimination from a complex in which the palladium sits at the benzylic carbon of the allyl fragment ($\mathbf{GS_B}$). This more highly-strained ground state was calculated to be 15.3 kcal/mol higher in energy than $\mathbf{GS_A}$, making it an improbable species in the reaction.[9] It was considered that instead of bond-formation, complex $\mathbf{GS_A}$ might dissociate one PPh_3 ligand to form three-coordinate palladium complex $\mathbf{GS_C}$. This ground state lies almost 22 kcal/mol lower in energy than $\mathbf{GS_A}$, and the barrier for its formation ($\mathbf{TS_C}$) is only 3.7 kcal/mol. These energies suggest that formation of complex $\mathbf{GS_C}$ from $\mathbf{GS_A}$ should be both rapid and thermodynamically favored, presumably driven by a loss of strain.

While calculations on the bis-ligated systems failed to indicate a potential origin for the experimentally observed linear product, they did point to complex $\mathbf{GS_C}$ as a reasonable intermediate. As a result, we considered potential pathways for bond-formation from this complex (Fig. 2). In line with the studies by Espinet,[5c] barriers for diene formation from this three-coordinate system were found to be lower overall than those found for the bis-ligated system (Fig. 1). From $\mathbf{GS_C}$, 3,3′-reductive elimination to give the

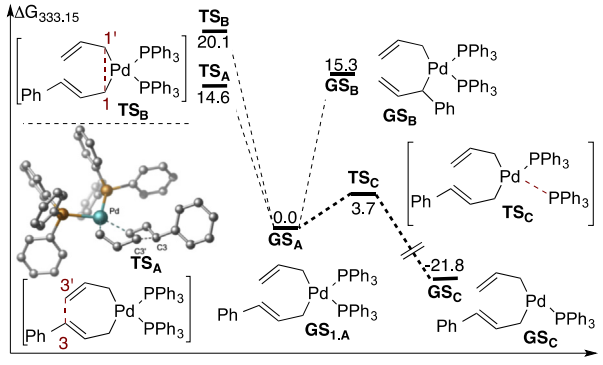

Fig. 1. Calculated activation free energy barriers (ΔG) in kcal/mol relative to $\mathbf{GS_A}$ (B3LYP-PCM(THF)/LANL2DZ(Pd)-6-31G**(C,H,P) (333.15 K).

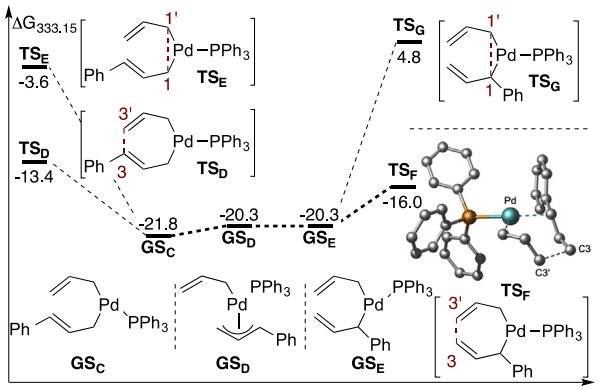

Fig. 2. Calculated activation free energy barriers (ΔG) in kcal/mol relative to $\mathbf{GS_A}$ (B3LYP-PCM(THF)/LANL2DZ(Pd)-6-31G**(C,H,P) (333.15 K). All energies include free PPh_3 to align with those shown in Fig. 1.

branched compound **3** ($\mathbf{TS_D}$, Fig. 2) was found to have a barrier of only 8.4 kcal/mol. The activation energy for 1,1′-reductive elimination to give linear product ($\mathbf{TS_E}$) was calculated to be 18.2 kcal/mol, now almost 10 kcal higher in energy than the 3,3′ ($\mathbf{TS_D}$). This result suggests that the 1,1′-pathway remains an improbable source of linear product for the three-coordinate system as well. Searching for an alternate explanation, we found the benzylic ground state ($\mathbf{GS_E}$) to be far less disfavored with only one ligand on the palladium, now only 1.5 kcal/mol higher in energy than $\mathbf{GS_C}$.[10] Excitingly, from this ground-state formation of linear product **4** via 3,3′-reductive elimination through $\mathbf{TS_F}$ was found to have a barrier of only 4.3 kcal/mol. Presumably by allowing the favored 3,3′-elimination to occur between two unsubstituted carbons, this activation free energy lies lower than any of the other barriers calculated for formation of either isomer of diene. Reaction through $\mathbf{TS_F}$ could represent the dominant source of the linear product in allyl-allyl couplings with monodentate ligands, and its low barrier compared to $\mathbf{TS_D}$ would explain why such high linear to branched ratios are observed experimentally with PPh_3.[11]

Although systems containing only one phosphine ligand should favor linear product formation ($\mathbf{TS_F}$, Fig. 2), the calculations also suggest that the branched product should be favored ($\mathbf{TS_A}$, Fig. 1) when two ligands are bound to Pd. If the mono- and bis-ligated complexes indeed give opposite regioselectivity, it appeared tenable that branched to linear ratios should be dependent on the equilibrium between these two complexes. To explore this idea experimentally, the Pd-catalyzed allyl-allyl coupling of cinnamyl carbonate **1** and allylB(pin) **2** was carried out with increasing equivalents of triphenylphosphine (Scheme 2). While the linear isomer **4** remained favored in all cases, entries 3 and 4 show that the amount of branched product **3** increased with higher equivalents of triphenylphosphine relative to Pd. In line with the computations suggesting that three-coordinate $\mathbf{GS_C}$ lay far below four-coordinate $\mathbf{GS_A}$, a large excess (10 equiv) of ligand was required to exceed even a 10:1 ratio of linear to branched product (entry 4). This experiment supports the idea that the linear isomer arises

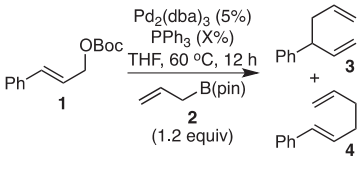

entry[a]	X (equiv.[b])	l:b (**4**:**3**)[c]
1	5 (.5)	>20:1
2	20 (2)	93:7
3	40 (4)	91:9
4	100 (10)	89:11

[a] >95% conversion in all cases.
[b] Relative to Pd.
[c] Determined by ^{1}H-NMR Analysis.

Scheme 2. Effect of added PPh_3 on allyl-allyl coupling.

from a three-coordinate complex, while the branched isomer might arise from a complex involving two phosphine ligands.

2.2. Bidentate ligands

Having established a tenable explanation for the linear selectivity observed with monodentate ligands, the effect of bidentate ligand bite-angle on regioselectivity was explored. We had originally proposed that small-bite-angle bidentate ligands gave high branched selectivity by separating the 1 and 1′ carbons, effectively slowing the 1,1′-elimination pathway and allowing the 3,3′-path to prevail. In contrast, a larger bite-angle ligand might increase the proximity of the 1 and 1′ carbons, allowing the 1,1′-reductive elimination to ensue. To probe this hypothesis computationally, the activation free energy barriers for both the 3,3′- and 1,1′-reductive elimination pathways were calculated for four of the ligands shown in Table 1. Interestingly, the calculations provide little correlation between elimination barriers and ligand bite-angle (Fig. 3). Each of the ligands showed $\Delta\Delta G^{\ddagger}$ values favoring the 3,3′-pathway by >11 kcal/mol relative to the 1,1′-path. These results fail to provide a link between ligand bite-angle and the variability in regioselectivity observed experimentally, and suggest that an alternate explanation is required.

Considering other pathways that could lead to the linear coupling product, we considered whether large-bite-angle ligands might allow reaction through three coordinate 'arm off' complexes akin to **TS$_F$** as proposed for monodentate ligands. In this context, factors other than bite-angle such as ligand flexibility could also play a role in regiocontrol. As flexibility is often unrelated to ligand bite-angle,[6,12] this feature might explain the nonlinear correlation between bite-angles and branched to linear ratios (e.g., entries 5–8, Table 1). To examine this effect, the experiment shown in Scheme 3 was carried out.[13] While structurally similar to bidentate dppf, di-*tert*-butylphenylferrocene (D*t*-BPF) has been shown to act as a hemilabile or monodentate ligand in Pd-catalyzed cross-couplings.[14] Accordingly, when employed in the allyl-allyl coupling of cinnamyl electrophiles and allylB(pin) (Scheme 3), D*t*-BPF gives a nearly opposite branched to linear ratio relative to dppf (15:85 vs 96:4). Assuming that D*t*-BPF is able to act as a hemilabile ligand in this reaction as well, these results suggest that the lowered regioselectivity could arise from a competition between palladium complexes in which one or both of the phosphines of the bidentate ligand are coordinated.

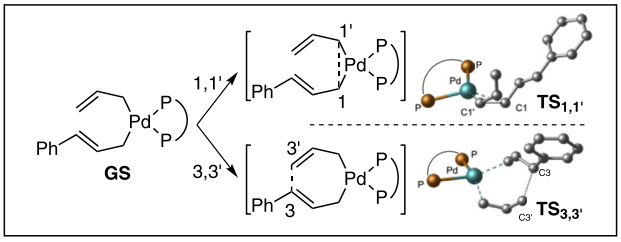

entry	Ligand	β_n[a]	b:l[b]	$\Delta G^{\ddagger}$ 3,3'[c]	$\Delta G^{\ddagger}$ 1,1'[c]	$\Delta\Delta G^{\ddagger}$[d]
1	dppe	85°	98:2	17.7	33.2	15.7
2	dppf	96°	96:4	12.4	26.9	14.5
3	dppb	98°	38:62	17.9	29.7	11.8
4	DPEphos	102°	72:28	13.9	27.9	14.0
5	xantphos	111°	53:47	12.6	27.5	14.9

[a] Natural bite-angle (see ref. 6). [b] Branched:linear ratio as determined experimentally. [c] Calculated activation free energy barrier (ΔG) in kcal/mol at 333.15K (B3LYP-PCM(THF)/LANL2DZ(Pd)-6-31G**(C,H,P,O). [d] Calculated as $\Delta G^{\ddagger}$ 1,1'-$\Delta G^{\ddagger}$ 3,3'.

n = 1 **dppe**
n = 3 **dppb**
R = Ph **dppf**
R = *t*-Bu **D*t*-BPF**
DPEphos
xantphos

Fig. 3. Calculated reductive elimination selectivity from L_2Pd(allyl)(cinammyl) complexes with varied ligand bite-angle.

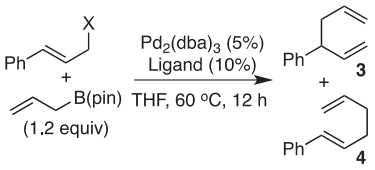

Ligand	X	b:l (3:4)[a]
dppf	OBoc	96:4
D*t*-BPF	Cl	15:85

[a] Determined experimentally by ^{1}H-NMR. >95% conv.

Scheme 3. Effect of Bis(phosphino)ferrocene ligand on allyl-allyl coupling.

To explore computationally the ability of larger-bite-angle ligands to act as hemilabile ligands (Fig. 4), xantphos (53:47 b:l, entry 8, Table 1) was chosen as a model ligand due to its structural rigidity and nonselectivity in coupling reactions. Overall, these computations indicated that xantphos may be able to access a similar pathway leading to linear diene formation as that proposed for triphenylphosphine. Starting from bis-ligated, bis(η^1-allyl) **GS$_F$**, 3,3′-reductive elimination through **TS$_H$** to give branched product occurs with an activation free energy barrier of 12.6 kcal/mol. The 1,1′-pathway (**TS$_I$**) is almost 15 kcal/mol higher in energy, and remains an improbable source of linear product. As an alternate to bond formation, **GS$_F$** can instead dissociate one arm of the phosphine ligand to give mono-ligated **GS$_G$**, which lies only 3.4 kcal/mol higher in energy. From this three-coordinate complex, 3,3′-reductive elimination through **TS$_J$** ($\Delta G^{\ddagger}$=10.0 kcal/mol) would also furnish the branched diene product.

As seen with triphenylphosphine (**GS$_C$** to **GS$_E$**, Fig. 2), **GS$_G$** can alternately isomerize to give **GS$_I$**, which lies 3.1 kcal/mol higher in energy than **GS$_G$**, presumably due to increased steric interactions between the adjacent phenyl substituent and the dissociated arm of the ligand. From this complex, 3,3′-reductive elimination (**TS$_K$**) to form linear product showed a relatively small barrier of only 4.4 kcal/mol, giving $\Delta\Delta G^{\ddagger}$ values of −1.7 and −2.5 kcal/mol relative to **TS$_H$** and **TS$_J$**, respectively. Assuming that the reaction is under Curtin-Hammett control, these calculations point to reaction through the mono-ligated **TS$_K$** as not only possible, but preferred. It should be noted that the relative calculated energies predict a much lower branched to linear ratio than is observed experimentally; however, the actual product ratio values are likely within the error of the calculated energy values, as **TS$_H$**, **TS$_J$** and **TS$_K$** all lie within 2.5 kcal/mol of one another. These calculations serve as qualitative evidence that large-bite-angle, flexible ligands may behave as hemilabile structures and allow reaction through three-coordinate complexes. This proposal could also explain why dppb, a flexible ligand with a bite-angle (98°) smaller than that of the more-rigid DPEphos or xantphos (102° and 109°, respectively) furnishes less branched product (entries 6–8, Table 1).

3. Conclusion

Overall, this study provides insight into how ligands control regioselectivity in allyl-allyl couplings. Although previous proposals considered small-bite-angle bidentate ligands to promote high branched selectivity by controlling rates of 3,3′- versus 1,1′-reductive elimination, the present study provides evidence of an alternate pathway. We now propose that the linear diene product is instead formed through a 3,3′-reductive elimination from a mono-ligated complex (**F**, Scheme 4) in which Pd sits at the substituted carbon of the allyl fragment. This explanation accounts for the high linear selectivity observed with monodentate ligands, and also provides a rationale for why large-bite-angle bidentate

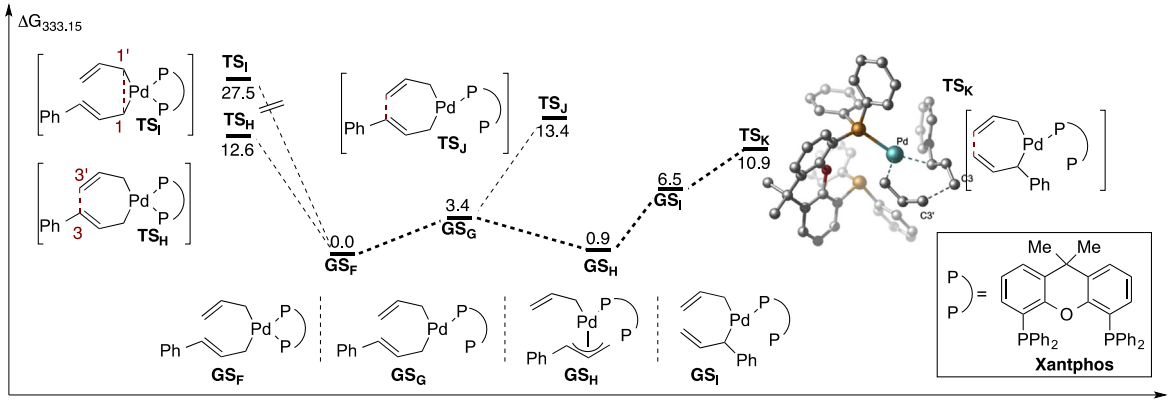

Fig. 4. Calculated activation free energy barriers (ΔG) in kcal/mol relative to **GS$_F$** (B3LYP-PCM(THF)/LANL2DZ(Pd)-6-31G**(C,H,P) (333.15 K).

bisphosphine ligands show inconsistent results. It is clear that ligand flexibility may play a significant role in controlling regioselectivity in allyl-allyl couplings, and may be an overlooked factor in related transition-metal catalyzed processes as well.

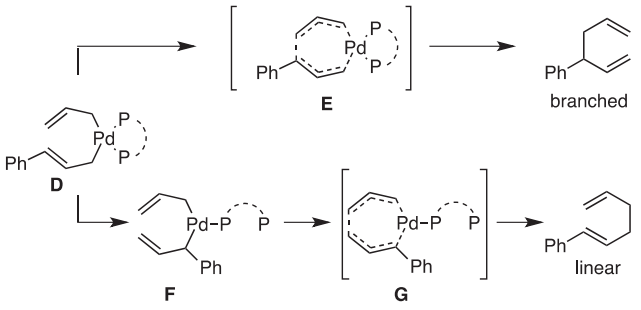

Scheme 4. Lowest energy paths to linear and branched products.

4. Experimental

4.1. General

^{1}H NMR spectra were recorded on a Varian Unity Inova 500 (500 MHz). Liquid Chromatography was performed using forced flow (flash chromatography) on silica gel (SiO_2, 230×450 Mesh) purchased from Silicycle. Thin Layer Chromatography was performed on 25 μm silica gel plates purchased from Silicycle. Visualization was performed using ultraviolet light (254 nm), potassium permanganate ($KMnO_4$) in water. All reactions were conducted in oven-dried glassware under an inert atmosphere of argon. Tetrahydrofuran (THF) was purified using a Pure Solv MD-4 solvent purification system from Innovative Technology Inc. by passing through two activated alumina columns after being purged with argon. Tris(dibenzylideneacetone) dipalladium(0) [$Pd_2(dba)_3$], tripheylphosphine (PPh_3), 4,5-Bis(diphenylphosphino)-9,9-dimethylxanthene (Xantphos), and 1,1′-bis(ditertbutylphosphino)ferrocene (D*t*-BPF), were purchased from Strem Chemicals, Inc. All other reagents were purchased from either Fisher or Aldrich and used without further purification.

4.2. Preparation of 1a[15]

A flame-dried round-bottomed flask equipped with a magnetic stir bar was charged with THF (30.0 mL) and cinnamyl alcohol (1.34 g, 10.0 mmol) under a nitrogen atmosphere. The solution was cooled to −78 °C, and *n*-butyl lithium (10 mmol, 4.8 mL of a 2.1 M solution) was added dropwise over a period of 10 min, and the solution was stirred at −78 °C for 30 min. A separately prepared solution of di-*tert*-butyl dicarbonate (2.18 g, 10.0 mmol) dissolved in 5 mL of THF under a nitrogen atmosphere was added dropwise at −78 °C, and the solution was warmed to 0 °C for 2 h followed by gradual warming to room temperature overnight. The reaction was re-cooled to 0 °C and quenched with diethyl ether and ice water (100 mL of a 3:2 mixture), poured into a separatory funnel and extracted into diethyl ether (3×100 mL). The combined organics were dried over magnesium sulfate, filtered, and concentrated in vacuo. The crude reaction mixture was purified on silica gel (10:1 pentane:diethyl ether) to afford a clear, colorless oil (1.78 g, 76% yield). R_f=0.60 (10:1 pentane:diethyl ether, stain in $KMnO_4$) Spectral data are in accordance with the literature.

4.3. Cross-coupling in Table 1 with PPh_3

An oven-dried two-dram vial equipped with magnetic stir bar was charged with $Pd_2(dba)_3$ (1.1 mg, 1.25 μmol), triphenylphosphine (PPh_3) (1.3, 5.2, 10.4 or 26.2 mg; 5.0, 20, 40.0 or 100 μmol), and THF (0.2 mL) in a dry-box under argon atmosphere. The vial was capped and stirred for five minutes, then *tert*-butyl cinnamyl carbonate (23.4 mg, 0.100 mmol) was added, followed by allylboronic acid pinacol ester (20.2 mg, 0.120 mmol). The vial was sealed, removed from the dry-box, and allowed to stir at 60 °C for 12 h. After this time, the reaction mixture was diluted with diethyl ether, filtered through a plug of silica gel and concentrated in vacuo. The branched:linear product was determined by ^{1}H NMR, spectral data for the branched[3a] and linear[16] products (**3** and **4**) are in accord with the literature.

4.4. Computational details

All calculations were performed using Gaussian 09 with all geometry optimizations, energies and frequencies calculated at the DFT level utilizing the B3LYP hybrid functional.[17,18] The 6-31G** basis set was used for the elements C, H, P, B, F and O in conjunction with the LANL2DZ relativistic pseudopotential for Pd and Fe. All free energies were calculated at 333.15 K or 273.15 K. The PCM model was used to estimate the effect of solvation (THF).[19] The frequency calculations for transition states demonstrated one imaginary frequency each, and each general transition state was found to connected with the correct ground states through IRC calculations. NBO analysis was carried out with Gaussian NBO version 3.1.[20] The three-dimensional structures presented in the figures were visualized utilizing CYLview.[21]

Acknowledgements

Frontier Scientific is acknowledged for generous donations of allylB(pin). The NIH (GM-64451) is acknowledged for financial

support. MJA acknowledges support in the form of fellowships from the American Chemical Society (DOC) and AstraZeneca.

Supplementary data

Experimental and computational procedures and data are included as Supplementary data. Supplementary data associated with this manuscript can be found in the online version. Supplementary data related to this article can be found at http://dx.doi.org/10.1016/j.tet.2015.05.015.

References and notes

1. Negishi, E.-I.; Liao, B. In *Handbook of Organopalladium Chemistry for Organic Synthesis*; Negishi, E.-I., de Meijere, A., Eds.; Wiley-Interscience: West Lafayette, IN, 2002; Vol. 1, pp 591–596.
2. For nonselective or linear selective allyl-allyl couplings, see: (a) Trost, B. M.; Keinan, E. *Tetrahedron Lett.* **1980**, *21*, 2595; (b) Godschalx, J.; Stille, J. K. *Tetrahedron Lett.* **1980**, *21*, 2599; (c) van Heerden, F. R.; Huyser, J. J.; Williams, D. B. G.; Holzapfel, C. W. *Tetrahedron Lett.* **1998**, *39*, 5281; (d) Nakamura, H.; Bao, M.; Yamamoto, Y. *Angew. Chem., Int. Ed.* **2001**, *40*, 3208; (e) Flegeau, E. F.; Schneider, U.; Kobayashi, S. *Chem.—Eur. J.* **2009**, *15*, 12247; (f) Jiménez-Aquino, A.; Flegeau, E. F.; Schneider, U.; Kobayashi, S. *Chem. Commun.* **2011**, 9456 For intramolecular allyl-allyl couplings, see: (g) Trost, B. M.; Pietrusiewicz, K. M. *Tetrahedron Lett.* **1985**, *26*, 4039; (h) Cuerva, J. M.; Gómez-Bengoa, E.; Méndez, M.; Echavarren, A. M. *J. Org. Chem.* **1997**, *62*, 7540 For related couplings, see: (i) Keinan, E.; Peretz, M. *J. Org. Chem.* **1983**, *48*, 5302; (j) Keinan, E.; Bosch, E. *J. Org. Chem.* **1986**, *51*, 4006.
3. (a) Zhang, P.; Brozek, L. A.; Morken, J. P. *J. Am. Chem. Soc.* **2010**, *132*, 10686; (b) Zhang, P.; Le, H.; Kyne, R. E.; Morken, J. P. *J. Am. Chem. Soc.* **2011**, *133*, 9716; (c) Brozek, L. A.; Ardolino, M. J.; Morken, J. P. *J. Am. Chem. Soc.* **2011**, *133*, 16778; (d) Le, H.; Kyne, R. E.; Brozek, L. A.; Morken, J. P. *Org. Lett.* **2013**, *15*, 1432 For related allyl-allenyl couplings see: (e) Ardolino, M. J.; Morken, J. P. *J. Am. Chem. Soc.* **2012**, *134*, 8770; (f) Ardolino, M. J.; Eno, M. S.; Morken, J. P. *Adv. Synth. Catal.* **2013**, *355*, 3413 For related Ir- and Cu catalyzed couplings to furnish branched 1,5-dienes, see: (g) Hornillos, V.; Pérez, M.; Fañanás-Mastral, M.; Feringa, B. L. *J. Am. Chem. Soc.* **2013**, *135*, 2140; (h) Hamilton, J. Y.; Sarlah, D.; Carreira, E. M. *J. Am. Chem. Soc.* **2014**, *136*, 3006; (i) Hamilton, J. Y.; Hauser, D.; Sarlah, D.; Carreira, E. M. *Angew. Chem., Int. Ed.* **2014**, *53*, 10759.
4. Ardolino, M. J.; Morken, J. P. *J. Am. Chem. Soc.* **2014**, *136*, 7092.
5. (a) Méndez, M.; Cuerva, J. M.; Gómez-Bengoa, E.; Cárdenas, D. J.; Echavarren, A. M. *Chem.—Eur. J.* **2002**, *8*, 3620; (b) Cárdenas, D. J.; Echavarren, A. M. *New J. Chem.* **2004**, *28*, 338; (c) Perez-Rodriguez, M.; Braga, A. A. C.; de Lera, A. R.; Maseras, F.; Alvarez, R.; Espinet, P. *Organometallics* **2010**, *29*, 4983.
6. The bite-angles as presented are the 'natural bite-angles' of the ligands, see: (a) van Leeuwen, P. W. N. M.; Kramer, P. C. J.; Reek, J. N. H.; Dierkes, P. *Chem. Rev.* **2000**, *100*, 2741; (b) van Leeuwen, P. W. N. M.; Kramer, P. C. J.; Reek, J. N. H. *Pure Appl. Chem.* **1999**, *71*, 1443.
7. Portions of this work have been published in the thesis of MJA. See: Ardolino, M. J. *Synthesis of Enantioenriched 1,5- Dienes and 1,5-Enynes by a Palladium-catalyzed 3,3-Reductive Elimination: Methodology Development and Mechanistic Studies* Ph.D. Dissertation; Boston College: Chestnut Hill, MA, 2014.
8. For references detailing the use of DFT for distinguishing between transition states leading to regio- and stereoisomers in related allylic substitutions, see: (a) Keith, J. A.; Behenna, D. C.; Mohr, J. T.; Ma, S.; Marinescu, S. C.; Oxgaard, J.; Stoltz, B. M.; Goddard, W. A., III. *J. Am. Chem. Soc.* **2007**, *129*, 11876; (b) Keith, J. A.; Behenna, D. C.; Sheridan, N.; Mohr, J. T.; Ma, S.; Marinescu, S. C.; Nielsen, R. J.; Oxgaard, J.; Stoltz, B. M.; Goddard, W. A., III. *J. Am. Chem. Soc.* **2012**, *134*, 19050; (c) Yamamoto, Y.; Takada, S.; Miyaura, N. *Organometallics* **2009**, *28*, 152.
9. The 3,3′ and 1,1′-pathways from this complex were considered, however, calculations failed to converge.
10. NBO analysis of GS_E also shows some donation of electron density from the adjacent arene into unfilled orbital of the Pd, suggesting that such an interaction might also help to stabilize this more-hindered ground state.
11. In addition to the pathways discussed that are operative through 3,3′- or 1,1′-couplings, there exists an additional η^3-η^1 pathway that might also account for the linear selectivity. The activation barriers for these couplings were calculated to be substantially higher than the 3,3′- or 1,1′- barriers discussed. See Supplementary data.
12. Casey, C. P.; Whittaker, G. T. *Isr. J. Chem.* **1990**, *30*, 299.
13. It was necessary to use cinnamyl chloride as the electrophile in the coupling with D*t*-BPF due to a significant amount of background reaction with the t-butoxide produced from carbonate 1.
14. Kawatsura, M.; Hartwig, J. H. *J. Am. Chem. Soc.* **1999**, *121*, 1473.
15. Adapted from: Trost, B. M.; Fraisse, P. L.; Ball, Z. T. *Angew. Chem., Int. Ed.* **2002**, *41*, 1059.
16. Radomkit, S.; Sarnpitak, P.; Tummatorn, J.; Batsomboon, P.; Ruchirawat, S.; Ploypradith, P. *Tetrahedron* **2011**, *67*, 3904.
17. Frisch, M. J.; Trucks, G. W.; Schlegel, H. B.; Scuseria, G. E.; Robb, M. A.; Cheeseman, J. R.; Scalmani, G.; Barone, V.; Mennucci, B.; Petersson, G. A.; Nakatsuji, H.; Caricato, M.; Li, X.; Hratchian, H. P.; Izmaylov, A. F.; Bloino, J.; Zheng, G.; Sonnenberg, J. L.; Hada, M.; Ehara, M.; Toyota, K.; Fukuda, R.; Hasegawa, J.; Ishida, M.; Nakajima, T.; Honda, Y.; Kitao, O.; Nakai, H.; Vreven, T.; Montgomery, J. A., Jr.; Peralta, J. E.; Ogliaro, F.; Bearpark, M.; Heyd, J. J.; Brothers, E.; Kudin, K. N.; Staroverov, V. N.; Kobayashi, R.; Normand, J.; Raghavachari, K.; Rendell, A.; Burant, J. C.; Iyengar, S. S.; Tomasi, J.; Cossi, M.; Rega, N.; Millam, J. M.; Klene, M.; Knox, J. E.; Cross, J. B.; Bakken, V.; Adamo, C.; Jaramillo, J.; Gomperts, R.; Stratmann, R. E.; Yazyev, O.; Austin, A. J.; Cammi, R.; Pomelli, C.; Ochterski, J. W.; Martin, R. L.; Morokuma, K.; Zakrzewski, V. G.; Voth, G. A.; Salvador, P.; Dannenberg, J. J.; Dapprich, S.; Daniels, A. D.; Farkas, Ö.; Foresman, J. B.; Ortiz, J. V.; Cioslowski, J.; Fox, D. J. *Gaussian 09, Revision A.02*; Gaussian: Wallingford CT, 2009.
18. (a) Becke, A. D. *Phys. Rev. A* **1988**, *38*, 3098; (b) Lee, C.; Yang, W.; Parr, R. G. *Phys. Rev. B* **1988**, *37*, 785.
19. (a) Miertus, S.; Scrocco, E.; Tomassi, J. *Chem. Phys.* **1981**, *55*, 117; (b) Barone, V.; Cossi, M.; Tomassi, J. *Chem. Phys.* **1997**, *107*, 3210.
20. NBO Version 3.1. Glendening, E. D.; Reed, A. E.; Carpenter, J. E.; Weinhold, F..
21. Legault, C. Y. *CYLview, 1.0b*; Université de Sherbrooke, 2009; http://www.cylview.org.